Octagon Rings Antennas for Compact Dual-Polarized Aperture Array

Yongwei Zhang, *Member, IEEE,* and Anthony. K. Brown, *Senior Member, IEEE*

***Abstract*—A wideband dual-polarized aperture antenna array is presented based on elements formed by pairs of octagonal rings. The octagon ring elements are linked by capacitors and kept a defined distance from a ground plane. A broader frequency bandwidth has been achieved by placing a further layer of conductive elements above the array forming a meta-material layer. Expanded polystyrene foam is used to fill the space between the array rings and the ground, and between the elements and the meta-material layer. Capacitive coupling can be realized by interdigitating the end portions of the rings. The parametric study of the proposed structure is presented. A variety of element shapes in the same arrangement have been investigated and the scan performance are compared. The octagon rings antenna array exhibits a broad element pattern with a low cross polarization in the wide scan range. The overall structure is low cost, compact and easy to fabricate.**

***Index Terms*—Aperture array, octagon, cross polarization, phased array.**

I. Introduction

MUnk has shown that an array of dipoles closed to a ground plane and linked by capacitors can have a very wideband active impedance [1] with a low cross polarization across a wide usable frequency bandwidth. This structure forms a Current Sheet Array(CSA) [2].

CSA intentionally utilizes the mutual coupling between the array elements [3], controlling the overall input impedance by introduction of capacitance between the adjacent elements. The impedance stability over the frequency band and scan angles is enhanced by placing dielectric layers on top of the dipole array. The superimposed dielectric layers are important to the design of the CSA. In this paper elements with non-dipole shapes but new element layout are employed which show enhanced performance and allow ready integration of dual polarization. Furthermore, a meta material layer forming the same pattern as the array elements has been placed over the array to replace the layers of dielectric slabs. The overall height of the array can be considerably reduced therefore a tightly packed array is formed. An equivalent frequency bandwidth can be obtained by using a parallel meta material layer with predetermined shapes and a relative distance to the main array elements. The element is preferably octagon rings in pairs and it is named as Octagon Rings Antenna (ORA).

Y. Zhang and Prof. A. K. Brown are with the School of Electrical and Electronic Engineering, The University of Manchester, Manchester, M60 1QD, U.K. e-mail: david.zhang@ieee.org, anthony.brown@manchester.ac.uk.

Manuscript received March 24, 2009; revised April 06, 2009 and September 13, 2009. This effort/activity is supported by the European Community Framework Programme 6, Square Kilometre Array Design Studies (SKADS), contract no 011938.

This paper is organized as follows: In Section II, the new design with different element shapes is introduced. Section III describes a new approach to use interdigitated capacitors to control the coupling between the ORA elements. The finite ORA is analyzed in Section IV while Section V gives the cross polarization properties. The measured active element pattern and scanned array patterns are investigated in Section VI. Section VI concludes the paper.

II. Overview of element types

A. Current Sheet Array

It is reported that an array of dipoles close to a groundplane can achieve a bandwidth of around 4:1 with a VSWR of less than 2:1 [4]. However, the inter-element spacing must be small, much less than a half wavelength at the high frequency. For applications where minimum number of elements are required, the largest spacing(that is the element spacing avoiding grating lobes at maximum scan angle at the highest frequency) between the elements is desired. For a CSA antenna the bandwidth is limited when the largest spacing is used. An example model of CSA by using closely spaced dipole elements has been given in [4]. The configuration considered consists of 2 layers of dielectric material on top of the dipole array in addition to two thin sheets on both sides to embed the dipole elements. Further investigations revealed that the layers of dieletric slabs can be replaced by an array of conductive patches with predetermined shapes and a relative distance from the array elements. The new structure is shown in Fig. 1. The scan performance of the infinite arrays for a dipole array of layered dieletric materials and the same array structure by merely replacing the dielectric slabs with the array of conducting patches is shown in Fig. 2. The size of the unit cell for comparison here is 150 mm and the distance from the main antenna sheet to the groundplane is 100 mm. The overall height of the array with 2 layers of dielectric meterial or a meta material layer is 200 mm and 150 mm respectively.

It is noted that the dipole array with the reflection meta layer shows a narrower bandwidth for the H-plane scans. In addition the element separation is limited to a half wavelength at the highest frequency. Therefore elements with non-dipole shapes including square, circle and octagon have been investigated. The unit cell of the optimised shape of octagon and octagon ring antenna is shown in Fig. 3, where L_g is the distance from the element array to the groundplane and h the distance from the meta material layer to the element array. The performances for these structures are dicussed in the following sections.

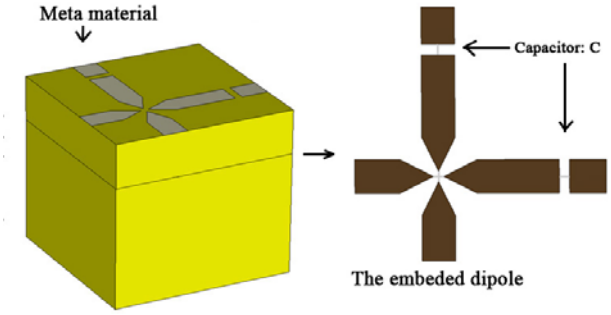

Fig. 1. The unit cell for a current sheet array with predetermined reflection conducting material on the top.

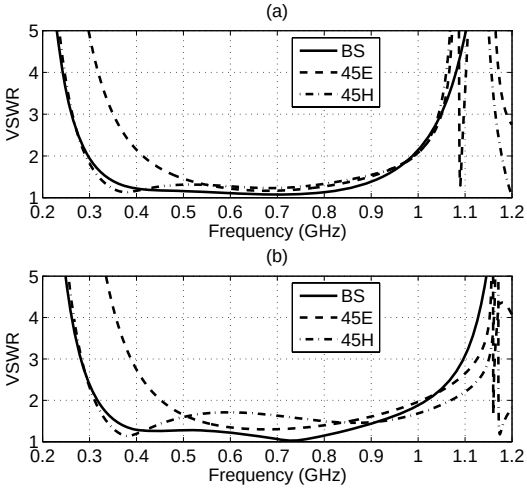

Fig. 2. The scan performance for an infinite current sheet dipole array, the element spacing is 150 mm, the distance from the array elements to the groundplane is 100 mm, (a) Two layers of dielectric material for reflection; (b) The displaced meta material for reflection, the distance from the array elements to the meta material layer is 40 mm.

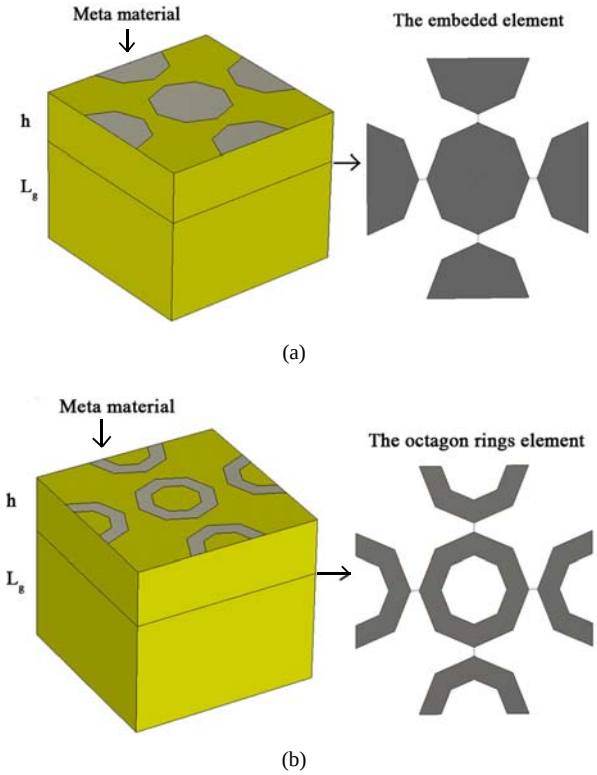

Fig. 3. The unit cell of the octagonal antenna, (a) Octagonal patches, (b) Octagon Rings Antenna.

B. Square patch antenna

Initially the arms of the dipoles are replaced by square patches to extend the element separation for a compact aperture. Additionally a dual-polarized structure is constructed with the orthogonally polarized element incorporated by rotating 90° of the co-polarized element and displace it by half of the element spacing. A scaled down square patches are placed above the array following the same pattern as the main elements. The scale factor (sf) is defined as the ratio between the size of the reflection patch and the size of the patch for the element. The VSWR for the dual-polarized infinite square patch array is shown in Fig. 4a.

C. The circle element

The leg of the element is changed from a square to a circle. The VSWR for the dual-polarized array is shown in Fig. 4(b). The scan performance in the H-plane is improved for the circle patches than the square ones.

D. Octagon antenna element

The infinite array with the element formed by a pair of octagonal patches has been simulated. The VSWR for the dual-

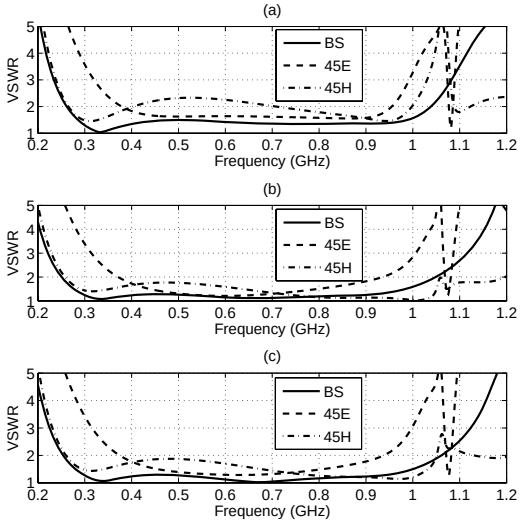

Fig. 4. The VSWR for the infinite dual-polarized arrays. (a) The square patch antenna array; (b) The circle patch antenna; (c) The octagon patch antenna.

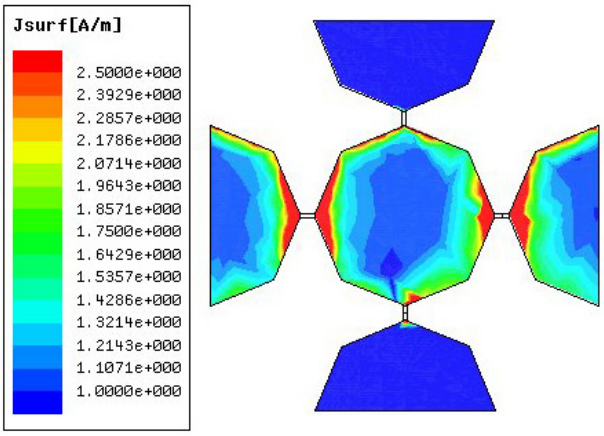

Fig. 5. The surface current at 700 MHz for broadside scan of an octagonal patch element in the infinite array.

Fig. 6. The prototype of 4×4 ORA finite array, the main element array is between the polystyrene foam slabs.

polarized thin octagonal patch antenna array is shown in Fig. 4(c). The surface current analysis reveals that the current flows along the edge of the octagonal patch. Further investigation indicates that the coupling between the orthogonal ports in a unit cell is reduced with a ring structure in pairs. The surface current of the element in an infinite array at 700 MHz for the broadside scan is shown in Fig. 5. It indicates that the current is concentrated along the edges of the element. Therefore an octagon ring antenna is presented. A 4×4 finite ORA array has been built before the large array fabrication and the mini-array is shown in Fig. 6. It can be seen that the array consists of the main element array between the two polystyrene foam slabs and the meta material layer on the top. The scan performance for an optimised ORA with the unit cell size of 165mm is shown in Fig. 7. The distance from the element array to the groundplane L_g=110 mm, the distance from the meta material layer to the element array h=70 mm, the ratio between the size of the reflection ring and the element ring is 0.94 and the coupling capacitance value is 1 pF.

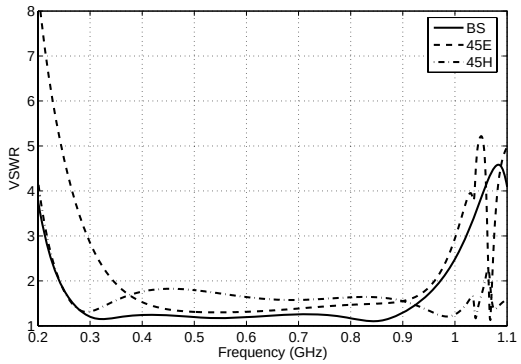

Fig. 7. Scan performance for an ORA, C=1pF, h=70 mm,L_g=110 mm, the scale factor sf=0.94, the size of the unit cell is 165 mm.

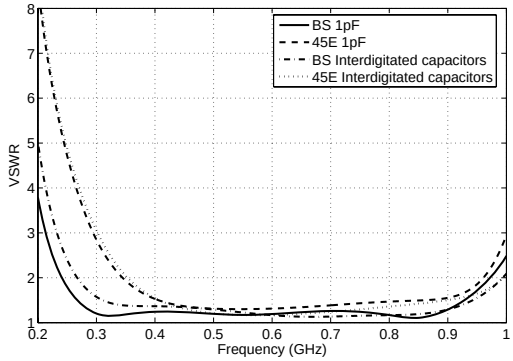

Fig. 8. The ORA with 1pF capacitor or interdigitated capacitors of 12 fingers, h=70 mm,L_g=110mm, sf=0.9 (a) 1pF capacitor; (b) Interdigitated capacitor with 12 fingers.

III. ORA ARRAY WITH FINGERING CONNECTIONS

The finite ORA was built and measured in a compact range. Bulk capacitors were soldered between the neighbouring ORA elements and this can be inconvenient in practice. The bulk capacitors can be replaced by interdigitating the spaced apart end portions to control the capacitive coupling between the adjacent ORA elements. The interlaced fingers are used to provide increased capacitive coupling. For the dual-polarized ORA array with 165 mm pitch size, the capacitors of 1 pF are needed. The capacitor can be built with 12 fingers with the length of the finger of 2.4 mm. The gap between the fingers is 0.15 mm. The scan performance comparison between the array using 1 pF bulk capacitor or the interdigitated capacitor with 12 fingers is shown in Fig. 8. The unit cell configuration is based on h=70mm, L_g=110mm, and sf=0.9. The array performances for these two coupling solutions are very close. The same unit cell with interdigitated capacitors configuration is simulated in both CST and HFSS. The active VSWR performance with scan from both CST and HFSS simulation are shown in Fig. 9. The agreement between the CST and HFSS simulations for the same array configuration is good.

IV. FINITE ORA ELEMENTS ARRAY

A 16×16 dual-polarized finite ORA was built and shown in Fig. 10. The ORA element is a balanced antenna and

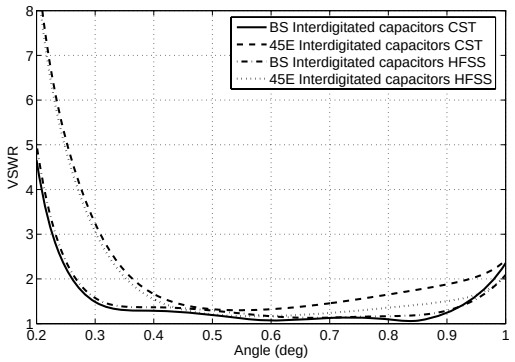

Fig. 9. The ORA with interdigitated capacitors of 12 fingers capacitor; (a) CST, (b) HFSS.

it requires a balanced feed. A balun has been designed to provide the transition between the unbalanced driven system and the balanced coplanar strip line connected to the adjacent rings for the element. The balun design is in accordance with the guidelines in [5]. The baluns to feed the ORA array is shown in Fig. 11. It is noted that the length of the balun is 120mm, however the distance between the array element to the groundplane is 100mm, therefore there is an extra part of the body of the balun reaching out of the groudplane. The radiated pattern of the centre element of the finite array has been measured in the presence of neighbouring elements. The rest elements surrounding the centre element are terminated with loads of 120 ohms. The element spacing is 165 mm and the capacitance value for the bulk capacitors between the elements is 1 pF. The overall height of the array is 150mm.

V. Element and Array Pattern

The "active" element pattern is measured for a single element (the elements near the centre of the array are chosen) with the rest of elements are terminated in matched loads [6]. The "active" element pattern has been preferably renamed as "scan" element pattern [7]. The scan element pattern is in general different from the radiation pattern for an isolated element. This is due to the mutual coupling effect between the neighbouring elements and the fed element. The scan element pattern can be assumed to be the same for each element in the array if the array is large enough.

For the 16×16 finite dual polarized ORA array fabricated, the co-polar and cross-polar scan element pattern for the centre element at three frequencies is shown in Fig. 12. It is seen that the scan element pattern is smooth and broad over E-, H- and D-planes without a significant ripple within the $\pm 45^\circ$ range. Although at high frequency of 1 GHz, minor ripples have been observed in this range. The cross-pol is 15 dB below the co-pol in the three planes.

In addition to the scan element pattern measurement, a subarray of 8×8 elements were used and the resulting scanned array pattern is shown in Fig. 13. The subarray has been scanned to three directions including broadside, 45° in the E-plane and 45° in the H-plane. The loss of gain with scan from broadside to 45° in these two planes is less than 1.5 dB with a slightly more scan loss in the E-plane than in the H-plane scans.

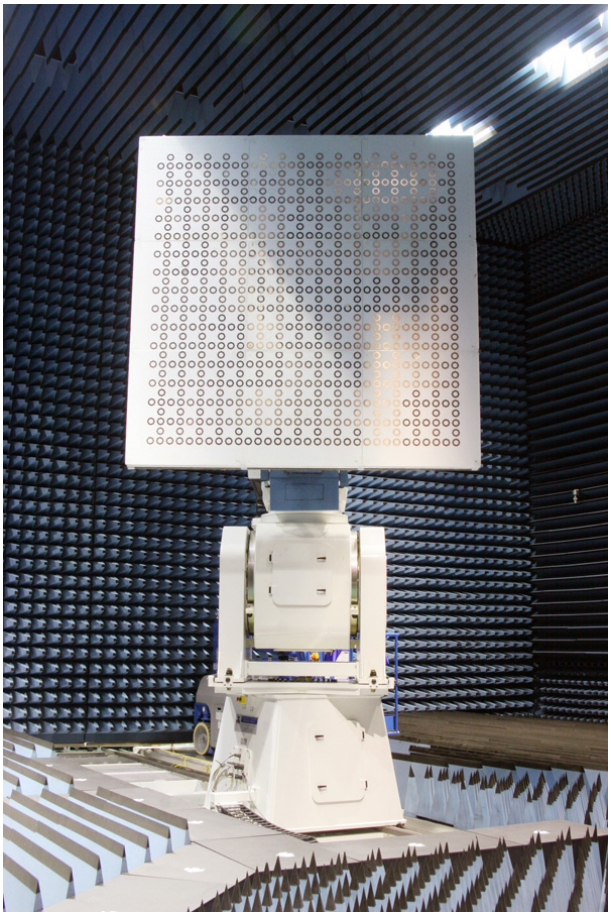

Fig. 10. The 16×16 finite ORA array, photo courtesy SELEX Galileo.

VI. Conclusions

A planar approach with a square grid for broadband aperture array antenna design has been presented. The octagonal ring elements is shown to have improved performance over other polygonal shapes of square or circle elements. The orthogonal-polarized components are incorporated by sharing one leg of the antenna with the copolar elements. The array can be fabricated by using two layers of conductive polygonal rings separated by polystyrene form and hence it is a cost effective and low profile solution for large scale arrays. To avoid the bandwidth reduction and loss associated with a balun, a balanced feeding scheme is recommended. The array can exhibite 4:1 bandwidth and the cross-polarization is 15 dB below the co-polarization within a $\pm 45^\circ$ scan range.

Acknowledgment

The authors would like to thank Tim Ikin and Georgina Harris for their efforts on the fabrication and measurement of the finite array.

References

[1] B. Munk, "A wide band, low profile array of end loaded dipoles with dielectric slab compensation," *Proceedings of the 2006 Antenna Applications Symposium, EuCAP 2006*, pp. 149–165, September 2006.

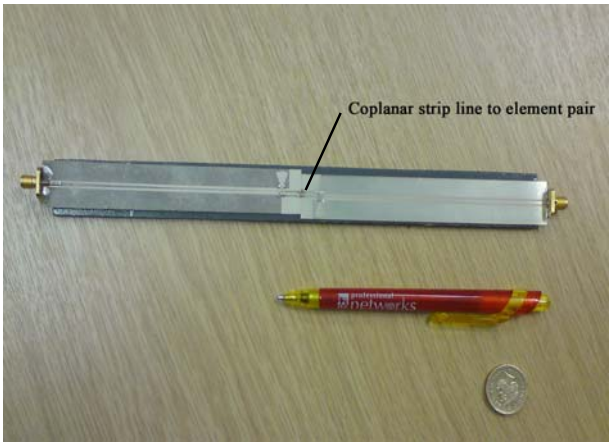

(a)

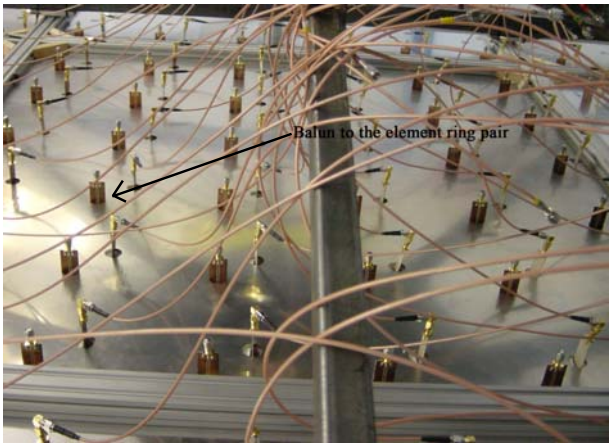

(b)

Fig. 11. The balun to feed the ORA array, (a) Two baluns in back to back configuration, (b) Baluns passing through holes in the groundplane to feed the ORA elements.

[2] H. A. Wheerler, "Simple relations derived from a phased-array antenna made of an infinite current sheet," *IEEE Trans. Antenna Propagat.*, vol. AP-13, no. 4, pp. 506–514, July 1965.

[3] B. Munk, *Finite Antenna Arrays and FSS*. John Wiley & Sons, 2003.

[4] B. Munk, R. Taylor, T. Durham, W. Croswell, B. Pigon, R. Boozer, . S. Brown, M. Jones, J. Pryor, S. Ortiz, J. Rawnick, K. Krebs, M. Vanstrum , G. Gothard, and D. Wiebelt, "A low-profile broadband phased array antenna," *Antennas and Propagation Society International Symp. 2003, IEEE*, pp. 448–451, June 2003.

[5] J. Thaysen, K. B. Jakobsen, and J. Appel-Hansen, "A wideband balun—how does it work?" *Applied Microwave & Wireless, Norcross, GA, USA, vol. 12(10)*, pp. 40–50, 2000.

[6] D. M. Pozar, "The active element pattern," *IEEE Trans. Antenna Propagat.*, vol. 42, no. 8, pp. 1176–1178, August 1994.

[7] R. C. Hansen, "Comments on "the active element pattern"," *IEEE Trans. Antenna Propagat.*, vol. 43, no. 6, p. 634, June 1995.

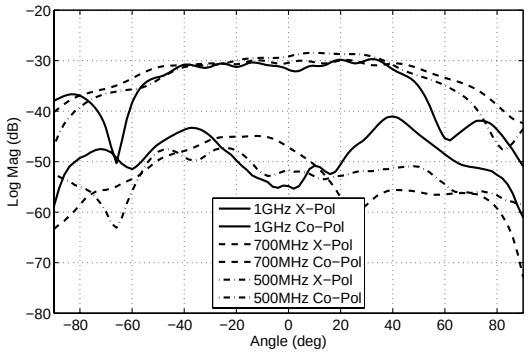

(a)

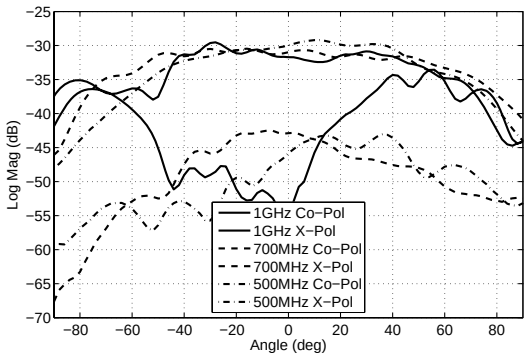

(b)

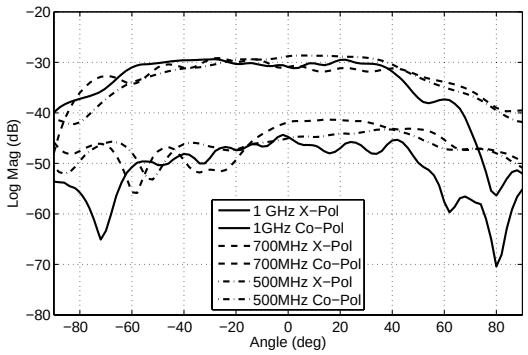

(c)

Fig. 12. The immersed centre element pattern of the 16×16 finite ORA array(a) E-plane, (b) D-plane, (b) H-plane.

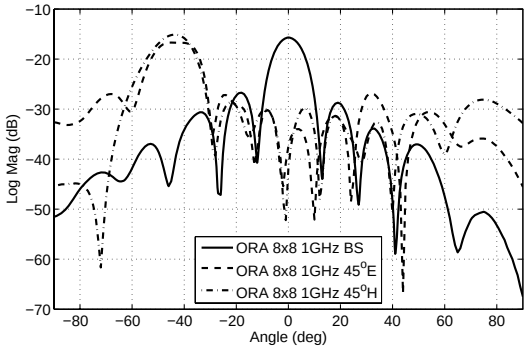

Fig. 13. Measured scanned beam pattern at 1 GHz for the finite ORA array.